



Effects of physical structure and processes on thin zooplankton layers in Mamala Bay, Hawaii

J. C. Sevadjan^{1,*}, M. A. McManus¹, G. Pawlak²

¹Oceanography Department, and ²Ocean Resources Engineering Department, University of Hawaii, Manoa, Honolulu, Hawaii 96822, USA

ABSTRACT: Vertically thin layers of zooplankton were found to be common and recurring features in Mamala Bay on the south shore of the island of Oahu, Hawaii. The formation, maintenance, and vertical displacement of these thin layers are, in part, a function of regional physical oceanographic processes. The purpose of this study was to quantify general thin zooplankton layer characteristics in Mamala Bay and the underlying physical environment in which they occurred. We utilized a 2 mo time series of acoustic backscatter measurements from a calibrated acoustic Doppler current profiler (ADCP) to identify thin scattering features; took biological samples; and collected vertical profiles of physical, optical, and biological characteristics of the water column. In general, thin zooplankton layers were associated with increased water column stability. Stratification at the study site was low relative to other coastal regions around the continental USA where thin layers have been observed. Instances of significant stratification were short-lived, and possibly as a result, thin layers were shorter in duration. Diurnal surface heating accounted for much of the observed stratification, and the breakdown of stratification during civil twilight corresponded with a decrease in thin zooplankton layer formation. Biological and optical measurements taken during a focused shipboard profiling experiment over the course of the study suggested a mechanism for zooplankton layer formation in which zooplankton converged to graze on a thin phytoplankton layer.

KEY WORDS: Thin layer · Physical processes · Stratification · Zooplankton

Resale or republication not permitted without written consent of the publisher

INTRODUCTION

Observational studies of the coastal ocean over the past few decades have shown that the distribution patterns of plankton communities in these environments are highly complex. Organisms respond both passively and actively to fine-scale changes in their environments. Understanding the interconnectivity between the organisms and the physical, chemical, and biological characteristics of their habitats is critical to understanding how their distributions evolve.

Research on plankton dynamics has shown that small-scale variability, or 'patchiness', is a very important part of the dynamics of marine ecology. Advances in instrument technology and sampling methods have revealed the tendency of some marine organisms to converge into dense, vertically thin structures. These 'thin layers' contain extremely high concentrations of

organisms and thus represent loci of biological and chemical processes. The partitioning of organisms in the vertical can dramatically affect the ecology of the regions in which they occur, affecting feeding, larval survival, behavior, and predation by higher trophic levels (McManus et al. 2003). Despite being only a few centimeters to a few meters in thickness, thin layers have been observed to be horizontally coherent for kilometers, and persist for up to several days. Continuing research has shown that these features are not at all uncommon; they have been observed and studied across a wide variety of ocean environments and were found to be recurring features (Nielsen et al. 1990, Donaghay et al. 1992, Cowles & Desiderio 1993, Dekshenieks et al. 2001, Holliday et al. 2003, McManus et al. 2005, Cheriton et al. 2007, Sullivan et al. 2010a).

Prior studies have shown that the formation, maintenance, and dissipation of thin layers are related to

*Email: sevadja@hawaii.edu

changes in the underlying physical environment. Thin layers are often found in conjunction with vertical gradients of some physical property, such as water density or current velocity. Franks (1992) and Stacey et al. (2007) proposed a buoyancy-driven mechanism for thin layer formation in which non-motile, or passive, organisms settle at densities equal to their own density; therefore one would expect a higher concentration of organisms near large density gradients. This theory has been supported by observational work by Dekshenieks et al. (2001), who found that a large percentage (71 %) of thin layers were associated with the pycnocline. Another purely physical mechanism that has been proposed to contribute to thin layer formation is strain by a sheared velocity profile (Franks 1995, Stacey et al. 2007). To this end, Ryan et al. (2008) found strong statistical relationships between shear in the water column and the presence of thin layers. Thus, an understanding of the regional physical processes that contribute to local stratification and shear may help to predict the occurrence of conditions that are favorable to thin layer development and maintenance.

In addition, motile species of phytoplankton and zooplankton can actively converge into thin layers seeking nutrients, food, specific light intensities, sexual reproduction, or defense (Sullivan et al. 2010b). In some cases, zooplankton seem to expend considerable energy in maintaining their position within a layer, in spite of physical processes that would act to dissipate the layer (McManus et al. 2003). Although thin layers have been statistically associated with highly stable regions of the water column (Dekshenieks et al. 2001, Cheriton et al. 2007), evidence also suggests that organism swimming can overcome moderate amounts of turbulence in order to maintain the organisms' association with the layer (McManus et al. 2003). A biological mechanism for the formation of thin layers was proposed by McManus et al. (2003), in which foraging behavior aggregates zooplankton at depths occupied by higher abundances of phytoplankton and microzooplankton. It has become increasingly apparent that the dynamics of thin layers are likely to be a function of multiple physical and biological processes operating simultaneously.

We utilized time series of backscatter from a calibrated acoustic Doppler current profiler (ADCP) in Mamala Bay on the south shore of the island of Oahu, Hawaii, USA, to look for acoustic scattering features characteristic of thin zooplankton layers. Careful calibration of the ADCP was necessary to identify and distinguish these features. Building on our initial detection of thin layers on the south shore of Oahu, Hawaii, the primary objective of the present study was to provide a quantitative description of (1) the general characteristics of thin layers in Mamala Bay, and (2) the

physical conditions under which these layers were observed. The relative importance of the convergent and divergent mechanisms that result in thin layer formation is likely to vary across geographic regions. Thus, we focused this study on the physical structure and processes associated with thin zooplankton layers at a particular coastal site and provide a comparison of relevant processes across different coastal sites along the west coast of the USA. To supplement this physical analysis, trophic interactions during one thin layer were examined over the course of an overnight shipboard profiling experiment.

MATERIALS AND METHODS

Study area. Mamala Bay is located on the south shore of the island of Oahu, the third western-most of the main islands in the Hawaiian Archipelago, USA (Fig. 1). The bay is roughly 32 km in its east–west direction and 4.5 km in its across-isobath direction. Much of Mamala Bay is between 300 and 500 m depth. From these depths, the bathymetry slopes gently ($\sim 1^\circ$) shoreward. At the shelf break (between 2 and 3 km offshore) the bathymetry rises abruptly ($\sim 6^\circ$) from 200 m to 100 m depth. Shoreward of the 100 m isobath, the bathymetry again slopes gently ($\sim 1^\circ$) shoreward.

The study was located 0.4 km offshore of Kaka'ako Waterfront Park, between Honolulu Harbor and Ala Moana Beach Park, at the Kilo Nalu Ocean Observatory (Pawlak et al. 2009; www.soest.hawaii.edu/OE/KiloNalu/). The observatory provides power and data communications to a suite of instruments at 12 and 20 m water depth.

Time series of current velocity, acoustic backscatter, and temperature were measured by instruments at the 12 m node of the Kilo Nalu Observatory for a 10 wk period between 17 July and 26 September 2007 (Fig. 2) (Sansone et al. 2008). Additional temperature data were provided by a second thermistor chain deployed on the 40 m isobath. Within this time frame, an autonomous profiler (the ODIM SeaHorse; ODIM Brooke Ocean) was moored 250 m offshore of the 12 m node for 2 multiweek deployments. The autonomous profiler deployments provided a spatial context of the physical conditions throughout the water column. To supplement these time series, an overnight shipboard profiling experiment was conducted (90 m from the node) to examine the physical, biological, and optical structure of the water column at a very high vertical and temporal resolution. Direct sampling, with a 2.2 l water-sampling bottle and plankton net, was undertaken at the study site during one thin layer event.

Kilo Nalu 12 m node—current magnitude and direction. A 1228.8 kHz RD Instruments (RDI) ADCP

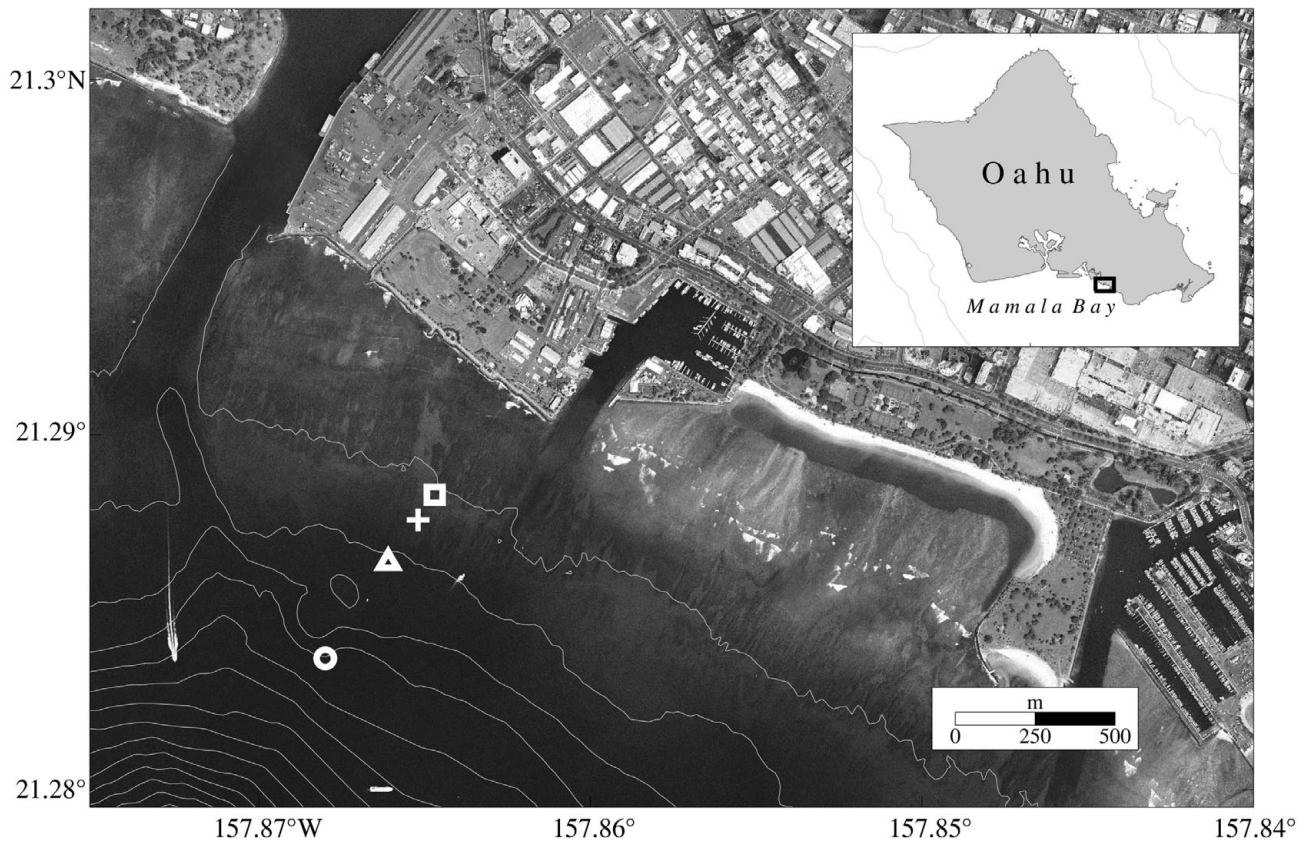


Fig. 1. Island of Oahu (1000 m and 2000 m depth contours shown; inset); and overhead view of study site from a geo-referenced aerial photograph, including instrument deployment locations. (□): Kilo Nalu Observatory 12 m node, which provided measurements of acoustic backscatter, current velocities, and temperature; (+): 24 h shipboard profiling experiment. (Δ): SeaHorse autonomous profiler; (○): 40 m thermistor chain site. White isobaths are plotted from 10 to 140 m depth, in 10 m increments. Image source: US Geological Survey

was deployed at the 12 m node of the Kilo Nalu Observatory throughout the duration of the study (Table 1). This ADCP was bolted to a heavily weighted frame on the seafloor in an upward-looking mode. This instrument provided velocity measurements between 0.67 m above the bottom (mab) and 10.42 mab (approximately 2 m below the surface), at a vertical resolution of 25 cm. The ADCP was configured to measure current velocity and acoustic backscatter profiles every second. The raw velocity data was converted to along- and cross-isobath velocity

components in reference to the 127° heading of the 10 m isobath. The 1 Hz current velocity data was then box-averaged to 200 s ensembles.

Kilo Nalu 12 m node—temperature. Time series of water temperature were collected using a Precision Measurement Engineering thermistor chain, with 1 m vertical separation between temperature sensors, from 0.85 to 6.85 mab. Measurements were taken at a sampling frequency of 0.25 Hz (4 s). The accuracy of these instruments is reported by the manufacturer to be within $\pm 0.01^\circ\text{C}$. A field test was conducted in which

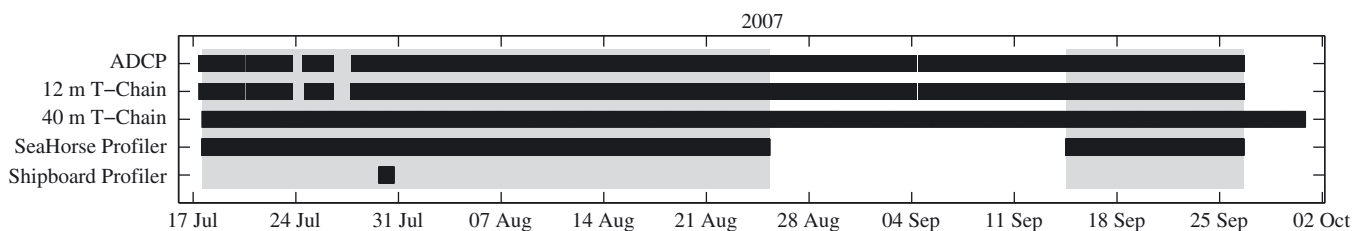


Fig. 2. Timeline of instrument deployments. Shaded gray regions represent the time period considered in the present study. ADCP: calibrated acoustic Doppler current profiler; 12 m T-Chain: thermistor chain at 12 m depth isobath; 40 m T-Chain: thermistor chain at 40 m depth isobath

Table 1. Instrumentation and sampling parameters utilized in study. ADCP: calibrated acoustic Doppler current profiler, DO: dissolved oxygen

Instrument	Manufacturer	Model	Measurement	Sampling frequency	Accuracy
Kilo Nalu 12 m node					
ADCP	RD Instruments	1228.8 kHz Workhorse Monitor	Current velocities; acoustic backscatter;	0.005 Hz (200 s) 1 Hz	1.0 cm s ⁻¹ ~3 dB
Thermistor chain	Precision Measurement Engineering	T-Chain	Temperature	0.25 Hz	±0.02°C
40 m site					
Thermistor chain	Sea-Bird Electronics	39	Temperature; pressure	0.033 Hz (30 s) 0.033 Hz (30 s)	±0.002°C 5 hPa
SeaHorse profiling package					
CTD	Sea-Bird Electronics	19plus	Temperature; conductivity; pressure	4 Hz 4 Hz 4 Hz	±0.005°C ±0.0005 S m ⁻¹ ±1.38 hPa
24 h shipboard profiling package					
CTD	Sea-Bird Electronics	25	Temperature; conductivity; pressure	8 Hz 8 Hz 8 Hz	±0.002°C ±0.0003 S m ⁻¹ ±3.44 hPa
DO sensor	Sea-Bird Electronics	43	Dissolved oxygen	8 Hz	2% of saturation
Fluorometer	WET Labs	WetStar	Chlorophyll; fluorescence	8 Hz	±0.03 µg l ⁻¹
Transmissometer	WET Labs	C-Star	Beam transmittance	8 Hz	±0.025 %

each of the thermistors was connected to the 12 m node and deployed at the same location. Results from this test indicated that the error of these instruments, when deployed at the observatory's 12 m node, was ±0.02°C.

40 m site—temperature. At the 40 m site, 6 Sea-Bird Electronics (SBE) model 39 thermistors were deployed on a thermistor chain, from 5 to 30 mab, with 5 m vertical spacing. Temperature measurements at the 40 m site were taken every 30 s. This sampling period was chosen to conserve battery power without significantly aliasing measurements of high frequency internal waves. SBE-39 thermistors have an initial accuracy of ±0.002°C and resolution of 0.0001°C.

Autonomous profiler. The SeaHorse autonomous profiler makes use of wave energy to power extended, high-resolution profiling of water properties. The mooring wire is anchored to the seafloor and the instrument package is left to collect autonomous upcast profiles of the water column. After ascent, the profiler uses wave energy to descend back to the bottom of the mooring line. Between profiles, the sensor package remains stationary at the bottom until the next sampling interval. The profiler was moored 250 m offshore of the 12 m node at a water depth of 23 m during 2 periods: 17 July to 25 August 2007, and 14 to 26 September 2007 (Fig. 2). High-resolution vertical profiles were collected every hour from 16 m depth to 1 m depth at an average ascent rate of 25 cm s⁻¹. A Sea-Bird model

19plus CTD on the profiler measured temperature, salinity, and pressure. Data were collected at a rate of 4 Hz, achieving a vertical resolution of about 8 cm.

Shipboard profiler. The fishing vessel 'Alyce C', 10 m in length, was positioned 90 m from the 12 m node, from 16:00 h 29 July to 04:00 h 30 July 2007. A slightly negatively buoyant profiling package (descent rate 15 cm s⁻¹) was lowered, free of ship motion, from the surface to 1 mab approximately every 2.5 min over this 12 h period. This profiling method resulted in 340 profiles.

A SeaBird model 25 CTD on the profiler measured temperature, salinity, and pressure. A SeaBird model 43 on the profiler measured dissolved oxygen. A WET Labs WetStar fluorometer on the profiler measured chlorophyll fluorescence, and a WET Labs C-Star transmissometer on the profiler measured beam transmittance at 660 nm. Data were collected at a rate of 8 Hz, achieving a vertical resolution of approximately 2 cm.

Layer samples. The Kilo Nalu Observatory's cabled data stream provided real-time profiles of volume scattering strength from the 1228 kHz RDI ADCP, which we monitored remotely for the presence of thin scattering features. A coherent thin layer of acoustic scattering was detected during this monitoring period, and within 2 h a small team was assembled at the study site aboard the research vessel 'Force 17'.

Using the real-time profiles of acoustic scattering from the 1228 kHz ADCP as a guide, discrete bottle samples were taken both above (at 6, 5, and 4 m above) and below (1 m below) the observed layer. A 2.2 l Aquatic Research Instruments point water sampling bottle, triggered by a weighted messenger, was used for this sampling (after McManus et al. 2008).

Additionally, a 335 μm Sea Gear Corp. plankton net was used to directly sample the thin layer. A mesh size of 335 μm was chosen to correspond with the minimum-sized object predicted to scatter off a 1228.8 kHz acoustic signal (Clay & Medwin 1977; Chap. 6). Pressure data were recorded at a distance of 0.3 m from the ring center with a pressure sensor on a SBE model 39 (accuracy ± 500 Pa), which verified that the net was towed directly through the depth of the layer. The net was towed at an average speed of 0.7 m s^{-1} for a period of 3.3 min. Of that time, the net was located in waters above the layer for 0.4 min and within the depths of the layer for 2.9 min. Scattering strength in these waters above the layer was ~ 10 dB lower than scattering within the depths of the layer. Thus, the net sample was likely a good representation of the organisms that comprised the layer.

Calibration of ADCP. Determining volume scattering strengths from the return echo of an ADCP pulse requires careful calibration. We calibrated our RDI Broadband Workhorse ADCP at the Applied Research Laboratory at the University of Texas at Austin, Lake Travis Test Station (LTTS), on 13 November 2007.

The goal of this calibration was to quantify the terms in the basic sonar equation for volume reverberation (Eq. 1), in order to convert raw received signal strength indicator (RSSI) data collected during the study to absolute volume scattering strength in decibels:

$$S_v = RL - SL + 20 \log_{10}(r) + 2\alpha r - 10 \log_{10}(c\tau/2) - 7.7 + DI \quad (1)$$

where S_v is volume scattering strength (dB), RL is reverberation level (dB/ μPa), SL is source level (dB/ μPa), r is range (m), α is sound absorption (dB m^{-1}), c is the speed of sound in seawater (m s^{-1}), τ is the transmit pulse length (m), and DI is the directivity index for a circular plane piston transducer (dB) (Urick 1975). This calibration followed the general procedures detailed in Benfield et al. (2001), Deines (1999), and Stokes & Greenlaw (2004), and involved precise measurements of receive sensitivity, source level, and beam pattern, for each transducer. The process for calibration is described in detail in Sevadjian (2008).

Briefly, receive sensitivity calibrations provided linear regression terms for each transducer that were used to convert raw RSSI data to RL in dB. The relationship between the ADCP drive voltage and acoustic SL was obtained by aligning each transducer with a

calibrated hydrophone (Naval Undersea Warfare Center/Underwater Sound Reference Division model E8) at the beam pattern maximum, and varying the input power supply. Because the ADCP was cabled during the study period, drive voltage was very nearly constant (± 0.5 V) throughout the study.

The slant range to the center of a depth cell is given by the equation:

$$r = \frac{b + \frac{l+d}{2} + (n-1)d + \frac{d}{4}}{\cos(\theta)} \quad (2)$$

where b is the blanking distance from the transducer head to the center of the first bin (m), l is the pulse length (m), d is the bin length (m), n is the depth cell number, and θ is the beam angle (Deines 1999). Changes in r at the study site attributed to varying speed of sound had a negligible effect on S_v (< 0.02 dB) and thus were not corrected for.

The absorption of sound in seawater (α) was calculated from Francois & Garrison (1982) as a function of temperature, salinity, depth, pH, and the frequency of the sound source. In this calculation, temperature and pressure were obtained from sensors on the ADCP transducer head; pH (8.2) and salinity (35.15) were assumed to be constants typical of the site. Values for α over the study period varied between 0.37 and 0.45 dB m^{-1} , depending on environmental conditions. It should be noted that this calculation applies to acoustic frequencies of 200 Hz to 1000 kHz, and is expected to be accurate to within about 10 % outside this range (i.e. at 1228.8 kHz) (Francois & Garrison 1982).

τ and DI were constant throughout the study. The speed of sound in seawater (c) was calculated using a constant salinity of 35 and the ADCP temperature measurement.

Identification of thin zooplankton layers. In order to identify thin zooplankton layers, a set of criteria was established to assure objective and consistent layer identification. First, S_v was calculated from the raw (1 Hz) RSSI data using Eq. (1) and averaged over the 4 ADCP beams at each depth cell. Decibel averages in this study were computed by first taking the mean of the linearized form of this unit, and then converting back to decibel. S_v was required to be more than 25 dB above the instrument noise level (a constant value of -87 dB determined during the calibration) $+1\text{SD}$ of the *in situ* scattering strength throughout the water column. In addition, the scattering feature was required to be < 5 m thick (after Dekshenieks et al. 2001) and present for at least 30 min (after Cheriton et al. 2007) to be considered a thin layer. A median filter was applied to eliminate the majority of the sporadic features. After these time-depth vector pairs were identified, the time series of S_v was evaluated at 6 h intervals for spatial and temporal coherence characteristic of thin zoo-

plankton layers. Each 6 h block of data was visualized in a time-depth rendering of volume scattering strength in a graphical user interface that was written to provide a final, user-controlled filtering of incoherent features. Scattering features whose upper vertical bounds intersected with the shallowest bin of the ADCP (~1.5 to 2.5 m below the water surface, depending on tidal height) were not included in this analysis. Acoustic return signals from these shallow depths were corrupted by sidelobe interaction with the sea surface, and were also likely affected by waves and bubble injection. Likewise, scattering strength calculations near the seafloor (closest to the transducers) may have been corrupted by ringing of the transducers. Scattering strength at the deepest 1 to 2 bins was typically 5 dB lower than in the waters directly above them. Although it was not possible to quantitatively distinguish acoustic scattering from zooplankton and from other sources (e.g. turbulent microstructure, sediment), biological and optical profiles as well as net tows, where available, suggested a biological origin to the acoustic scattering.

Estimation of buoyancy frequency and Richardson number. Squared buoyancy frequency (N^2) values were calculated as:

$$N^2 = \frac{-g}{\rho_0} \times \frac{d\sigma_t}{dz} \quad (3)$$

where g is gravitational acceleration, ρ_0 is the mean density, and $\sigma_t = [\rho(S, T, 0) - 1000 \text{ kg m}^{-3}]$, where $\rho(S, T, 0)$ is the density calculated from salinity (S) and temperature (T) values with pressure = 0 Pa (Pond & Pickard 1983). Temperature and salinity data collected during the overnight shipboard profiling experiment indicated that salinity accounts for ~20% of variations in $d\sigma_t/dz$ at the study site. Because salinity was not measured at the 12 m node, $d\sigma_t/dz$ was estimated by combining temperature measurements at the 12 m node with salinity measurements at the SeaHorse profiler site. For each temperature measurement, the SeaHorse data set was truncated to a time period of ± 1 h. The average values were then calculated for each of the salinity terms that appear in the vertical derivative of the equation of state. Using these averaged values, we obtained estimates of $d\sigma_t/dz$ at each temperature measurement.

There are 2 main sources for error in this estimation of N^2 . The first involves using averaged values for the salinity terms, as opposed to *in situ* values. This error was quantified by calculating N^2 at the SeaHorse profiler in 2 ways: (1) using *in situ* temperature and salinity measurements, and (2) using *in situ* temperature measurements and the averaged salinity values. The difference between N^2 calculated from these 2 methods was within $\pm 5.37 \times 10^{-5} \text{ rad}^2 \text{ s}^{-2}$ in 95% of the

profiler measurements. The second source of error involves differences in vertical salinity structure between the SeaHorse profiler and the study site (a distance of 250 m). This source of error was tested during the overnight shipboard experiment (when salinity data at the study site was available). To quantify this error, N^2 was calculated (1) using temperature and salinity measurements from the shipboard profiler, and (2) using temperature measurements from the shipboard profiler and the averaged salinity values from the SeaHorse profiler. The difference between N^2 calculated from these 2 sources was within $\pm 6.38 \times 10^{-5} \text{ rad}^2 \text{ s}^{-2}$ in 95% of these measurements.

Shear was calculated after Itsweire et al. (1989):

$$S^2 = \left(\frac{dU}{dz} \right)^2 + \left(\frac{dV}{dz} \right)^2 \quad (4)$$

where U and V are the along- and across-isobath current velocity components. To reduce instrument error in the calculation of S , 1 s current velocity profiles were box-averaged into 200 s ensembles. This choice of window size was a tradeoff between reducing ADCP error and risking smoothing of the development of turbulent structure. The minimum internal wave period during the shipboard profiling experiment was 200 s. Rapid temperature drops ($dT/dt < -0.15^\circ\text{C min}^{-1}$) did occur sporadically at the 12 m site, and while the onset of these events was sharp, fluctuations throughout the duration of these events were on time scales > 200 s. This averaging method reduced the ADCP velocity error to 1 cm s^{-1} . Shear (S) and N^2 were calculated using 1 m vertical bins ($dz = 1 \text{ m}$), and were combined to calculate the gradient Richardson number:

$$Ri = \frac{N^2}{S^2} \quad (5)$$

For consistency with S , N^2 was also box-averaged into 200 s ensembles.

RESULTS

Biological statistics

Thin zooplankton layers were recurring features at the study site. A total of 43 layers were identified over the 51 d study period, with at least one layer being present during 69% of the study period's civil days (00:00 to 24:00 h). Thin layers formed at all times of day, but the greatest percentage of the observed layers (60%) formed in the daytime hours (between 10:00 and 22:00 h). The average duration of all thin layers over the study period was 3.4 h, and the maximum duration was 11.4 h. The average thickness of each layer ranged from 0.65 to 1.62 m. Out of 43 layers observed, 42 had

an average depth in the lower half of the water column (>5.5 m from the surface), and the average layer depth for all thin layers was 8.6 m. All layers were displaced vertically by at least 2.5 m over their duration; the maximum displacement was 9.1 m. The average volume scattering strength within each layer ranged from -60.9 to -52.9 dB, and averaged -58.3 dB, significantly above the instrument noise level of -87 dB.

Physical statistics

The physical structure of the water column at the study site was often very weakly stratified. Any significant stratification we did observe at the 40 m site was caused by rapid, M_2 periodic decreases in bottom temperature. These cold bottom water pulses rarely propagated into the shallow (12 m) waters of Mamala Bay. In contrast, the majority of the thermal stratification at the 12 m site was caused by diurnal solar heating.

Buoyancy frequency at the autonomous profiler was highest in the daytime, indicating that thermal stratification is an important source of stability between the hours of 10:00 and 22:00 h, and that convective mixing is an important source of instability during the nighttime near the study site (Fig. 3).

For each of the 43 thin zooplankton layers observed during the 51 d study period, estimates of buoyancy frequency and Richardson number were computed above, within, and below the layer. Although definitive values of buoyancy frequency and Richardson number could not be obtained because of the absence of salinity data at the study site, estimates for these parameters were calculated.

The estimated buoyancy frequency at the depth of each thin layer, averaged over the duration of the layer, was positive for 40 of 43 layers. During the 3 layers in

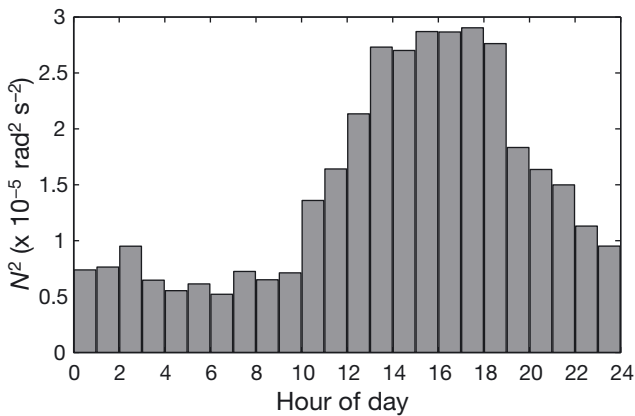


Fig. 3. Relationship between buoyancy frequency (N^2) and time of day over the 2 mo study

which the average estimated N^2 was negative, temperature measurements between thermistors at the 12 m thermistor chain were within the instrument error. Additionally, the average estimated buoyancy frequency at all depths was higher when thin layers were present (mean = $3.70 \times 10^{-5} \pm 1.12 \times 10^{-5} \text{ rad}^2 \text{ s}^{-2}$) than when no layers were present (mean = $1.77 \times 10^{-5} \pm 0.387 \times 10^{-5} \text{ rad}^2 \text{ s}^{-2}$) (Fig. 4). Bounds for these means represent 95% confidence intervals computed from t -tests of the N^2 data, and indicate that the difference between the 2 means is statistically significant.

The average calculated Richardson number at the depth of each of the 43 layers was $Ri = 0.615$. When thin layers were present, the average estimated Ri at all depths was statistically significantly higher (mean = 0.54 ± 0.07) than when no layers were present (mean = 0.30 ± 0.03).

Winds were predominantly out of the east during the study period. No significant changes in wind direction were observed over the study period. To investigate relationships between the surface and internal tide and the occurrence of thin layers, each hour of the study was scored for tidal height, semidiurnal tidal phase, number of days following full moon, and rate of change of bottom temperature at the 12 m site, along with the presence or absence of thin layers. For each of these physical variables, the data range was then divided into 10 equal bins, and the percentage of time that the data fell within each bin was calculated. This percentage was then compared to the percentage of the total number of thin layers that occurred within each bin.

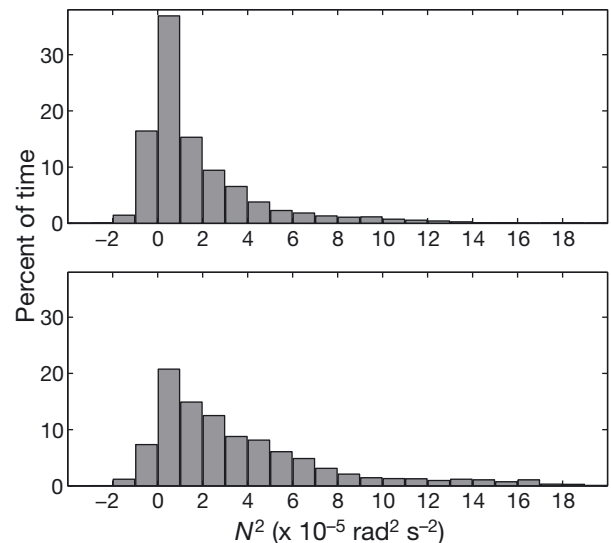


Fig. 4. Histogram of buoyancy frequency when thin layers were present (lower panel) and when no layers were present (upper panel). Thin layers generally persisted when stratification was higher than average

No distinct relationship between tidal height and thin layer occurrence was found during the present study. A slightly lower proportion of thin layers occurred within $\pm\pi/4$ radians of the high semidiurnal tide (17.4% of layers corresponding to 25.0% of the study time period). Proportionally more layers occurred during periods of quick drops in bottom temperature attributed to the internal tide of $dT/dt < -0.15^\circ\text{C min}^{-1}$ (25.1% of layers over 18.3% of the study time period). No clear relationship was found between lunar phase and thin layer occurrence.

Overnight shipboard profiling experiment

One thin acoustic scattering layer occurred during the 12 h shipboard profiling experiment (Fig. 5). The

layer appeared at 17:45 h and coincided with a pulse of cold, high-salinity bottom water, which was advected over the study site during ebb tide. The thin layer coincided with a strong density gradient ($d\sigma_t/dz$ approx. $-0.060 \text{ kg m}^{-3} \text{ m}^{-1}$) near the $22.73 \sigma_t$ isopycnal, and was located in a region of high buoyancy frequency ($N^2 > 3 \times 10^{-4} \text{ rad}^2 \text{ s}^{-2}$). The water at the layer depth was high in chlorophyll fluorescence, and there was a sharp decrease in oxygen levels at the depth of the layer following the dispersal of the layer (oxygen data for the first 3 h of the experiment were unavailable). Prior to the appearance of the layer, currents were strong throughout the water column and oriented along-isobath (towards the northwest); however, when the layer appeared, this fast-moving flow was restricted to the upper water column, and velocities at the depth of the layer were

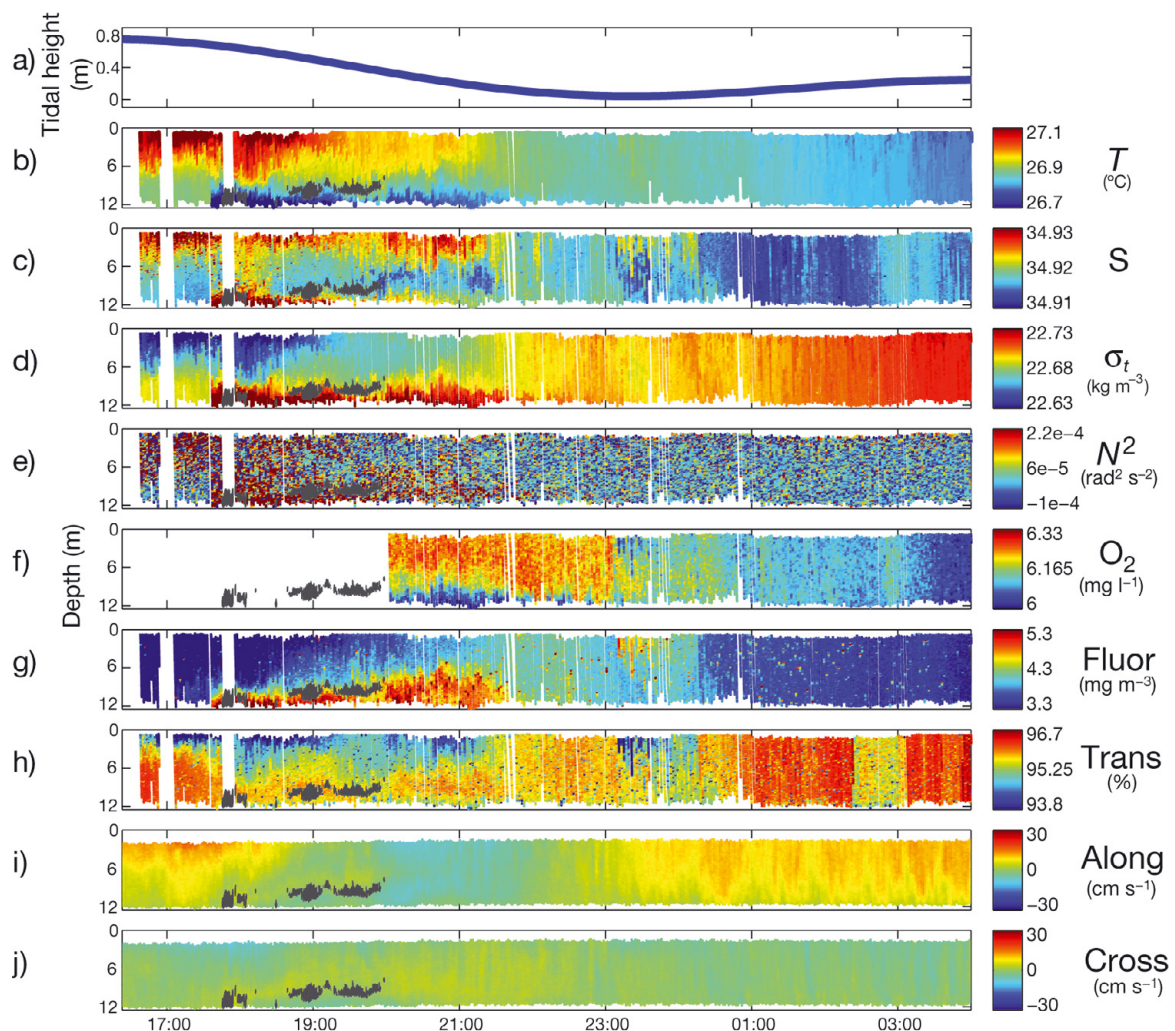


Fig. 5. Physical, optical, and biological data collected during the overnight shipboard profiling experiment (29 to 30 July 2007): (a) tidal height; (b) temperature (T); (c) salinity (S); (d) σ_t ; (e) buoyancy frequency (N^2); (f) dissolved oxygen (O_2); (g) chlorophyll fluorescence (fluor); (h) beam transmittance (trans); (i) along-isobath (NW[+] to SE[-], along); and (j) across-isobath (NE[+] to SW[-], cross) current velocity measured at the 12 m site. Black lines represent the trace of the thin layer identified from the acoustic scatter of the calibrated 1228 kHz ADCP at the 12 m site (for details see Fig. 1 & Table 1)

weak (mean = 1.9 cm s^{-1}) and oriented onshore. It should be noted that vertical velocities were slow ($<2 \text{ cm s}^{-1}$) throughout the profiling experiment. It is possible to interpret vertical velocities as the swimming speed of scattering organisms, due to the intrinsic property that ADCPs actually measure the speed of acoustic scatterers in the water, and not the water itself. Under this interpretation, no diel vertical movement of zooplankton was detected during the shipboard experiment.

The introduction of the dense bottom water into the study site caused the lower water column to be highly stable, while surface heating kept the upper water column stratified. At ~19:30 h, 1 h and 45 min after the first observation of the layer, the combination of cooling surface waters and persistent high salinity in the upper 6 m caused a decrease in stratification, with negative depth-averaged buoyancy frequencies. Inspection of volume scattering strength profiles indicated that shortly following this destratification the layer dispersed, and scatterers were distributed uniformly throughout the water column. From 21:30 h on 29 July to 04:00 h on 30 July, the water column was well-mixed (average $N^2 = -9.92 \times 10^{-8}$), and no thin layers were present.

Layer samples

While there are many advantages of using acoustics to look at organism distributions in the water column, one drawback of sampling acoustically with a single transmit frequency is that little information can be obtained about the identity of the scatterers. To identify the organisms present in thin zooplankton layers at the study site, direct samples were taken from one thin zooplankton layer. By remotely monitoring real-time profiles of acoustic scattering from the Kilo Nalu Observatory's calibrated 1228 kHz ADCP, we were able to identify a thin layer and equip a small research vessel at the site within 2 h. Using these real-time profiles as a guide, a net tow was taken at the depth of the zooplankton layer. Discrete water samples were also taken above and below the same layer. The bottle samples were almost entirely devoid of macroscopic particles and zooplankton. The plankton net sample taken through the layer yielded a wide variety and high concentration of organisms. Ninety percent of the net tow was dominated by 4 groups: calanoid and cyclopoid copepods, specifically the Cyclopoida genus *Oithona* (0.5 to 2.5 mm); mysid shrimp (4 to 6 mm); and chaetognaths (3.5 mm). No sediment particles were found in the net sample or in the bottle samples.

DISCUSSION

Biological statistics

Thin layers were present during 69% of the study period's civil days (00:00 to 24:00 h) in Mamala Bay. Cheriton et al. (2007) summarized thin zooplankton layer statistics at 4 sites along the west coast of the USA: East Sound, Washington; Cape Perpetua, Oregon; Monterey Bay, California; and Santa Barbara, California. The percentages of civil days (00:00 to 24:00 h) in which layers were present in these studies were 84, 38, 67, and 36%, respectively. Like at these sites, thin zooplankton layers in Mamala Bay are recurrent and significant features.

In Mamala Bay, thin zooplankton layers were observed to form at all times of day, but were more likely to form in the daytime (between 10:00 and 22:00 h). This is most likely the result of 3 processes: (1) increased phytoplankton biomass due to increased daytime growth, (2) settling of phytoplankton at density gradients caused by diurnal heating in the afternoon to early evening, and (3) behavioral response of larger, acoustically scattering organisms and zooplankton to actively key in on these concentrated food sources. A buoyancy-driven mechanism for thin phytoplankton layers was proposed by Franks (1992) and Stacey et al. (2007) in which non-motile or passive organisms/particles (e.g. some species of phytoplankton) settle by sinking, until reaching water of density equal to their own density. Capable swimmers, such as the organisms found in the net tow, may then congregate on the focused food supply to graze.

At the autonomous profiler site, buoyancy frequency was highest between 10:00 and 22:00 h, and lowest between 22:00 and 10:00 h. It is interesting to note that 60% of the layers formed during this more stable daytime period. This suggests that convective mixing may be an important mechanism in discouraging thin layers from forming in the late night to early morning in Mamala Bay. McManus et al. (2003) reported that thin layers can persist in regions of the water column where turbulence is moderate but insufficient to cause vertical mixing.

Thin layers at the study site persisted an average of 3.4 h, with a maximum duration of 11.4 h. In comparison, the average layer durations during the studies along the west coast of the USA were 14.52, 1.66, 6.85, and 3.38 h, at East Sound, Cape Perpetua, Monterey Bay, and Santa Barbara, respectively (Cheriton et al. 2007).

Due to the nature of their study, Cheriton et al. (2007) were able to collect extensive physical data at 2 of their sampling sites (East Sound and Monterey Bay) and limited physical data at 2 other sampling sites (Cape

Perpetua and Santa Barbara). For this reason, we will limit the further comparison of layers in Mamala Bay to layers observed by Cheriton et al. (2007) in East Sound and Monterey Bay.

Thin zooplankton layers and stratification

In general, stratification at the study site was lower compared to levels of stratification measured in East Sound and Monterey Bay. Several physical processes distinguish the present study site from other sites of thin layer studies, in terms of stratification. Hamilton et al. (1995) noted that the water in Mamala Bay is generally weakly stratified above 50 m depth even in the summer, when stratification is highest. Diurnal solar heating accounts for the majority of the thermal stratification in the shallow (12 m), nearshore waters of Mamala Bay. Although tidally driven cold bottom water pulses were common at the 40 m thermistor chain in Mamala Bay, they were less common at the 12 m site.

In East Sound, stratification is heavily influenced by the advection of freshwater plumes from river runoff outside the fjord (Dekshenieks et al. 2001, McManus et al. 2003). Thin zooplankton layers were often found at the density interface between buoyant, low salinity surface waters and deeper tidally driven flows (Dekshenieks et al. 2001, McManus et al. 2003).

The Monterey Bay study was conducted during persistent upwelling-favorable winds. During upwelling events, northern Monterey Bay rests in the shadow of the Santa Cruz mountains. The nearshore waters in this area are characterized by cold subsurface waters and a warm surface layer (4 to 7 m). This causes the water column to be highly stratified (Graham 1993, Woodson et al. 2007).

It is important to note that the processes that lead to stratification in the water column in East Sound and in Monterey Bay occurred over time scales of days to weeks, while the processes that lead to stratification in Mamala Bay occurred over time scales of hours. In Mamala Bay, thin layer persistence was on average shorter than the layers in East Sound by a factor of 4, and shorter than the layers in Monterey Bay by a factor of 2. This suggests that there could be a positive correlation between the persistence of stratification in the water column and the persistence of thin zooplankton layers.

In spite of the differences in the physical processes that lead to stratification in Mamala Bay, East Sound, and Monterey Bay, a result common to all of the sites was that thin layers occurred in waters of increased stratification. Throughout the present study in Mamala Bay, all of the layers observed were located in regions of the water column where the density profile (within instrument error) was stable ($N^2 > 0$).

Thin zooplankton layers and the Richardson number

It is generally accepted that the critical value of $Ri = 0.25$ is a useful guide for the prediction of dynamic stability of a stratified shear layer (Miles 1961, Scotti & Corcos 1972, Eriksen 1978). Values of $Ri > 0.25$ indicate a stable water column, while values of $Ri < 0.25$ indicate an unstable water column.

Prior studies have suggested that thin layers are more common in regions of the water column where $Ri > 0.25$ (Dekshenieks et al. 2001, McManus et al. 2005, Cheriton et al. 2007). Dekshenieks et al. (2001) observed a total of 119 phytoplankton thin layers in East Sound and found that all layers occurred in regions of the water column where $Ri > 0.23$. McManus et al. (2005) reported 7 thin zooplankton layers in Monterey Bay, each of which persisted only in regions of the water column where $Ri > 0.25$. In the present study, the average Richardson number for all 43 layers, within the depth range of the layer, was $Ri = 0.615$, indicating that these layers were forming in stable regions of the water column. Similar to other studies, when thin layers were present in Mamala Bay, the average estimated Richardson number at all depths was higher (average $Ri = 0.54$) than when no layers were present (average $Ri = 0.30$).

Overnight shipboard profiling experiment

One acoustic scattering layer was observed during our overnight shipboard profiling experiment. This shipboard experiment provided concurrent physical, biological, and optical data collected in conjunction with the thin acoustic scattering layer. During this 12 h profiling experiment, the observed layer was associated with low oxygen. Low oxygen could indicate a higher zooplankton biomass (via oxygen consumption). The layer was also located at a depth of increased chlorophyll fluorescence, indicating water with increased phytoplankton abundance. These observations suggest a model for the observed thin acoustic scattering layers in which (1) phytoplankton exhibit high biomasses in thin layers due to enhanced growth, behavior, and/or physical processes (Stacey et al. 2007) and (2) acoustically-scattering zooplankton congregate to these concentrated food sources to graze (McManus et al. 2003).

A particular physical process that might have contributed to this vertical layering of phytoplankton was an increase in stratification resulting from cold, high-salinity bottom water pulses. The layer we observed during the overnight shipboard profiling experiment coincided with cold, high-salinity water, and was located at a depth of strong density gradient ($d\sigma_t/dz$

approx. $-0.060 \text{ kg m}^{-3} \text{ m}^{-1}$). This again suggests that the density profile could play a key role in dictating the vertical distribution of plankton at the study site. Zooplankton scatterers were observed to be distributed evenly throughout the water column when stratification weakened $\sim 2 \text{ h}$ after sunset. It is possible that at this time the previously vertically concentrated phytoplankton spread out due to decreased stratification from cooling at the surface and convective mixing, and thus zooplankton had no cost advantage in remaining in a vertically compressed depth range. These observations underscore the link between processes controlling physical structure in the water column and the tendency of phytoplankton and zooplankton to form and persist in vertically concentrated layers.

CONCLUSIONS

Thin zooplankton layers were found to be recurring features on the south shore of the island of Oahu, Hawaii. The occurrence of these thin layers was strongly dependent on stratification in the water column. All of the layers observed were located in regions of the water column where the density profile (within instrument error) was stable ($N^2 > 0$). Additionally, buoyancy frequency and Richardson number were statistically significantly higher throughout the water column when thin layers were present than when no layers were present.

Stratification at the Mamala Bay study site was generally low relative to that of previous thin layer study sites. The stratification that was observed in Mamala Bay was mainly due to heating at the surface, and to the infrequent advection of cold bottom water. Our results, in comparison with studies of thin zooplankton layers at 4 sites along the west coast of the USA, indicate that in terms of thin layer formation, the time scales on which these stratifying processes occur may be related to the duration of thin biological layers.

The majority of the layers observed in this study occurred during the daytime, between 10:00 and 22:00 h. Time series of buoyancy frequency profiles indicated that convective mixing associated with nighttime cooling might be an important process discouraging thin layers from forming in the late evening to early morning.

High concentrations of phytoplankton were found within regions of high vertical density gradients. Passive organisms and particles (e.g. some species of phytoplankton) may settle by sinking, until reaching water of a density equal to their own density. If regions of the water column with large density gradients also have low dispersion forces, these types of settling thin layers could persist. Motile organisms (e.g. some spe-

cies of phytoplankton and zooplankton) may actively aggregate into stably stratified regions of the water column seeking nutrients, food, specific light intensities, sexual reproduction, or defense (Sullivan et al. 2010b). In agreement with other studies, we observed what appeared to be zooplankton grazing on a phytoplankton thin layer. This phytoplankton layer was vertically dispersed when surface cooling destabilized the water column.

Acknowledgements. We thank the principal investigators, technicians, and researchers in the Benthic Boundary Layer Geochemistry and Physics project; C. Greenlaw for leading the ADCP calibration and providing invaluable technical support and assistance with data analysis; A. Merritt, R. Smith, and B. Stokes for carrying out the ADCP calibration; K. Benoit-Bird, D. V. Holliday, D. McGehee, R. Lukas, E. Firing, and M. Merrifield for many helpful discussions; S. Grant for analyzing plankton samples; and J. Wells, B. McLaughlin, K. Millikan, J. Reich, D. Viviani, K. Stierhoff, A. Culley, P. Drupp, A. Fetherolf, K. Flanagan, and K. Selph for assistance in field work. This study was supported by the National Science Foundation grant NSF-0536616 (to G.P., M.A.M., E. De Carlo, F. Sansone, A. Hebert, T. Stanton).

LITERATURE CITED

- Benfield MC, McGehee DE, Keenan SF, Deines KL (2001) Calibration and use of a broadband ADCP to measure zooplankton volume scattering strengths. *J Acoust Soc Am* 109:2336
- Cheriton OM, McManus MA, Holliday DV, Greenlaw CF, Donaghay PL, Cowles TJ (2007) Effects of mesoscale physical processes on thin plankton layers at four sites along the west coast of the U.S. *Estuar Coasts* 30:575–590
- Clay CS, Medwin H (1977) *Acoustical oceanography: principles and applications*. John Wiley & Sons, New York, NY
- Cowles TJ, Desiderio RA (1993) Resolution of biological microstructure through in situ fluorescence emission spectra: an oceanographic application using optical fibers. *Oceanography* 6:105–111
- Deines KL (1999) Backscatter estimation using broadband acoustic Doppler current profilers. *Proceedings of the IEEE Sixth Working Conference on Current Measurement*, San Diego, CA
- Dekshenieks MM, Donaghay PL, Sullivan JM, Rines JEB, Osborn TM, Twardowski MS (2001) Temporal and spatial occurrence of thin phytoplankton layers in relation to physical processes. *Mar Ecol Prog Ser* 223:61–71
- Donaghay PL, Rines HM, Sieburth JMCN (1992) Simultaneous sampling of fine-scale biological, chemical and physical structure in stratified waters. *Ergeb Limnol* 36: 97–108
- Eriksen CC (1978) Measurements and models of fine structure, internal gravity waves, and wave breaking in the deep ocean. *J Geophys Res C* 83:2989–3009. doi: 10.1029/JC083iC06p02989
- Francois RE, Garrison GR (1982) Sound absorption based on ocean measurements. Part II: boric acid contribution and equation for total absorption. *J Acoust Soc Am* 72:1879–1890
- Franks PJS (1992) Sink or swim — accumulation of biomass at fronts. *Mar Ecol Prog Ser* 82:1–12
- Franks PJS (1995) Thin layers of phytoplankton: a model of formation by near-inertial wave shear. *Deep-Sea Res I* 42: 75–91

- Graham WM (1993) Spatio-temporal scale assessment of an 'upwelling shadow' in northern Monterey Bay, California. *Estuar Coasts* 16:83–91
- Hamilton PJ, Singer J, Waddell E (1995) Mamala Bay study, ocean current measurements: a report to the Mamala Bay Commission, HI. Technical report. Sci Appl Int Corp, Raleigh, NC
- Holliday DV, Donaghay PL, Greenlaw CF, McGehee DE, McManus MM, Sullivan JM, Miksis JL (2003) Advances in defining fine- and micro-scale pattern in marine plankton. *Aquat Living Resour* 16:131–136
- Itsweire EC, Osborn TR, Stanton TP (1989) Horizontal distribution and characteristics of shear layers in the seasonal thermocline. *J Phys Oceanogr* 19:301–320
- McManus MA, Alldredge AL, Barnard AH, Boss E and others (2003) Characteristics, distribution and persistence of thin layers over a 48 hour period. *Mar Ecol Prog Ser* 261:1–19
- McManus MA, Cheriton OM, Holliday DV, Greenlaw CF, Drake P (2005) Effects of physical processes on structure and transport of thin zooplankton layers in the coastal ocean. *Mar Ecol Prog Ser* 301:199–215
- McManus MA, Kudela RM, Silver MV, Steward GF, Sullivan JM, Donaghay PL (2008) Cryptic blooms: Are thin layers the missing connection? *Estuar Coasts* 31:396–401
- Miles JW (1961) On the stability of heterogeneous shear flows. *J Fluid Mech* 10:496–508
- Nielsen TG, Kiorboe T, Bjørnsen PK (1990) Effect of a *Chrysochromulina polylepis* subsurface bloom on the planktonic community. *Mar Ecol Prog Ser* 62:21–35
- Pawlak G, DeCarlo EH, Fram JP, Hebert AB and others (2009) Development, deployment, and operation of Kilo Nalu nearshore cabled observatory. *OCEANS-IEEE 2009 Conference, Bremen*. doi:10.1109/OCEANSE.2009.5278149
- Pond S, Pickard GL (1983) *Introductory dynamical oceanography*, 2nd edn. Butterworth-Heinemann, Oxford
- Ryan JP, McManus MA, Paduan JD, Chavez FP (2008) Phytoplankton thin layers caused by shear in frontal zones of a coastal upwelling system. *Mar Ecol Prog Ser* 354: 21–34
- Sansone FJ, Pawlak G, Stanton TP, McManus MA and others (2008) Kilo Nalu: physical/biogeochemical dynamics above and within permeable sediments. *Oceanography. Special Issue Coast Ocean Proc Obs Technol Mod* 21: 173–178
- Scotti RS, Corcos GM (1972) An experiment on the stability of small disturbances in a stratified free shear layer. *J Fluid Mech* 52:499–528
- Sevadjian JC (2008) The effects of physical structure and processes on thin zooplankton layers in Mamala Bay, Hawaii. MS thesis, University of Hawaii, Manoa, HI
- Stacey MS, McManus MA, Steinbuck JV (2007) Convergences and divergences and thin layer formation and maintenance. *Limnol Oceanogr* 52:1523–1532
- Stokes RH, Greenlaw CF (2004) Final report for long ranger ADCP calibrations on S/N 0825, 3813, and 5373. Prepared for Dr. Volker Strass. BAE Systems, San Diego, California
- Sullivan JM, McManus MA, Donaghay PL (eds) (2010a) The ecology and oceanography of thin plankton layers. *Contin Shelf Res Special Issue* 30(1):1–18
- Sullivan JM, Donaghay PL, Rines JEB (2010b) Coastal thin layer dynamics: consequences to biology and optics. *Cont Shelf Res* 30:50–65
- Urick RJ (1975) *Principles of underwater sound*, 2nd edn. McGraw-Hill, New York, NY
- Woodson CB, Eerkes-Medrano DI, Flores-Morales A, Foley M and others (2007) Diurnal upwelling driven by sea breezes in northern Monterey Bay: a local mechanism for larval delivery to the intertidal? *Contin Shelf Res* 27:2289–2302

*Editorial responsibility: Otto Kinne,
Oldendorf/Luhe, Germany*

*Submitted: October 2, 2009; Accepted: April 7, 2010
Proofs received from author(s): May 29, 2010*